

Towards nuclear reactions with coupled cluster theory

Gaute Hagen (ORNL)

Collaborators:

Thomas Papenbrock (UT/ORNL)

Morten Hjorth-Jensen (UiO/CMA/MSU)

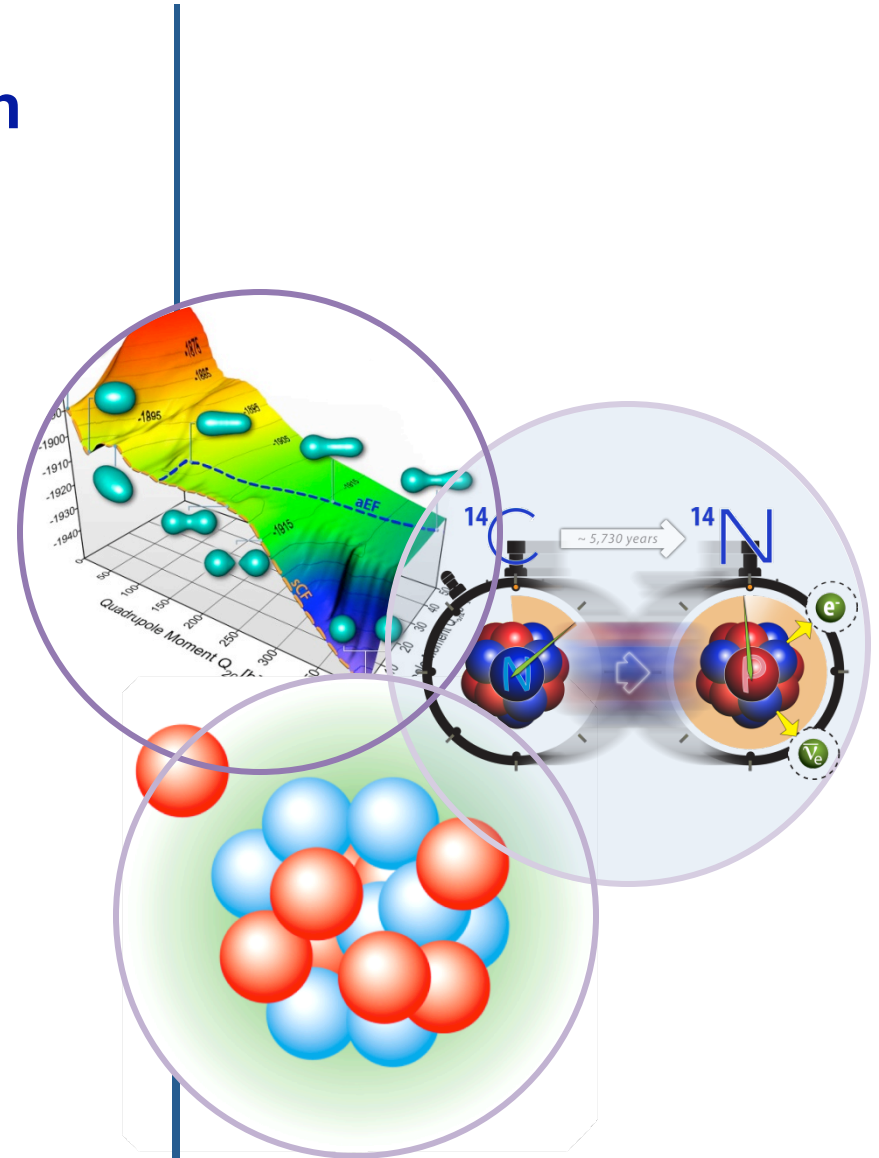
Gustav Jansen (UiO/CMA)

Ruprecht Machleidt (Idaho)

Nicolas Michel (UT/ORNL)

Nuclear Physics Seminar

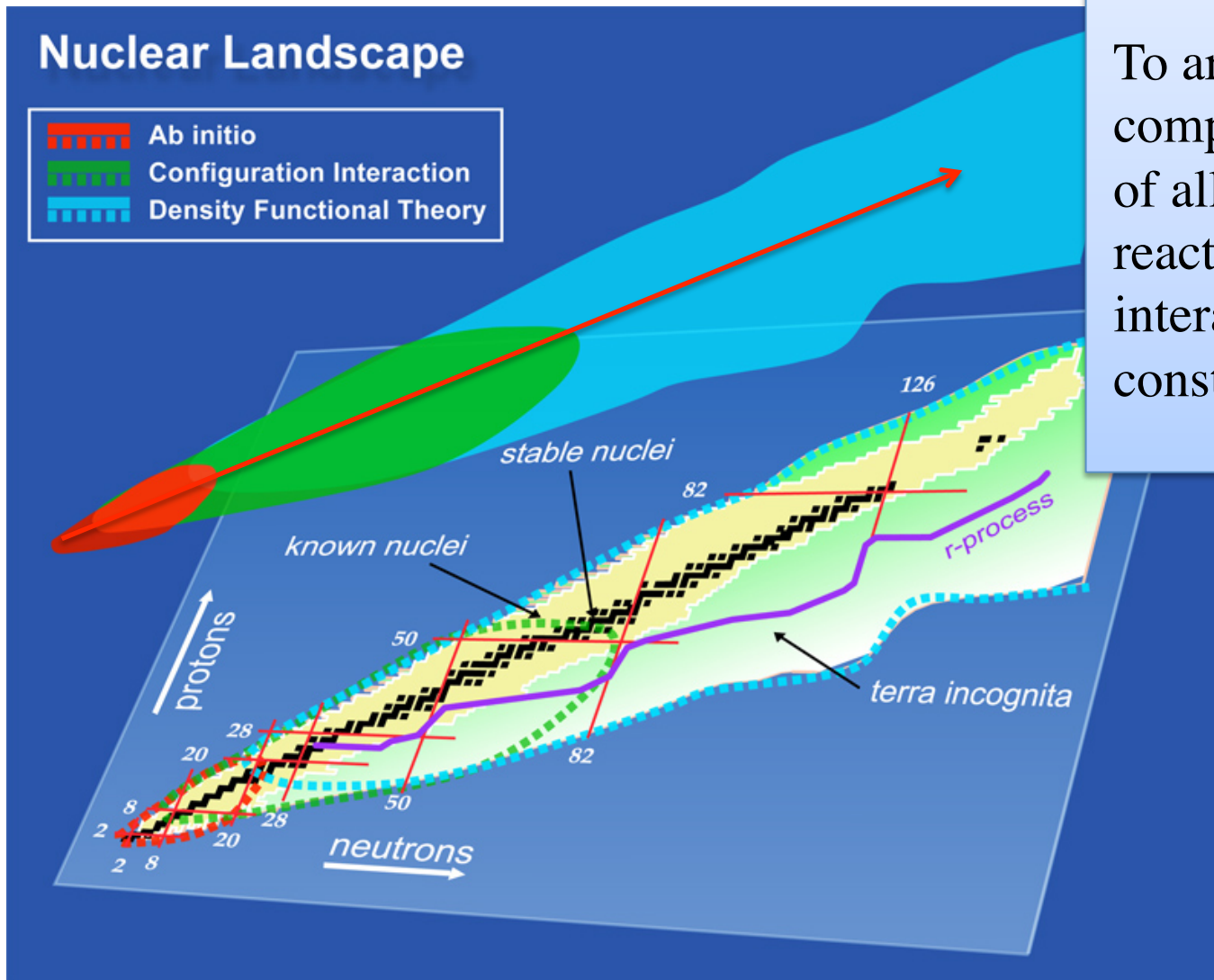
UT, February 20, 2012



Roadmap for Theory of Nuclei

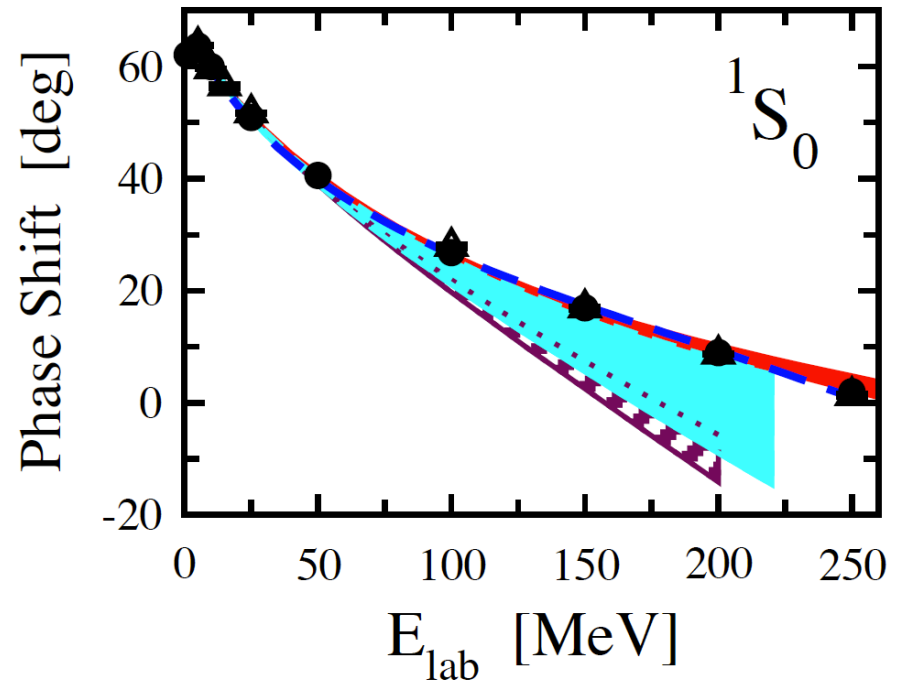
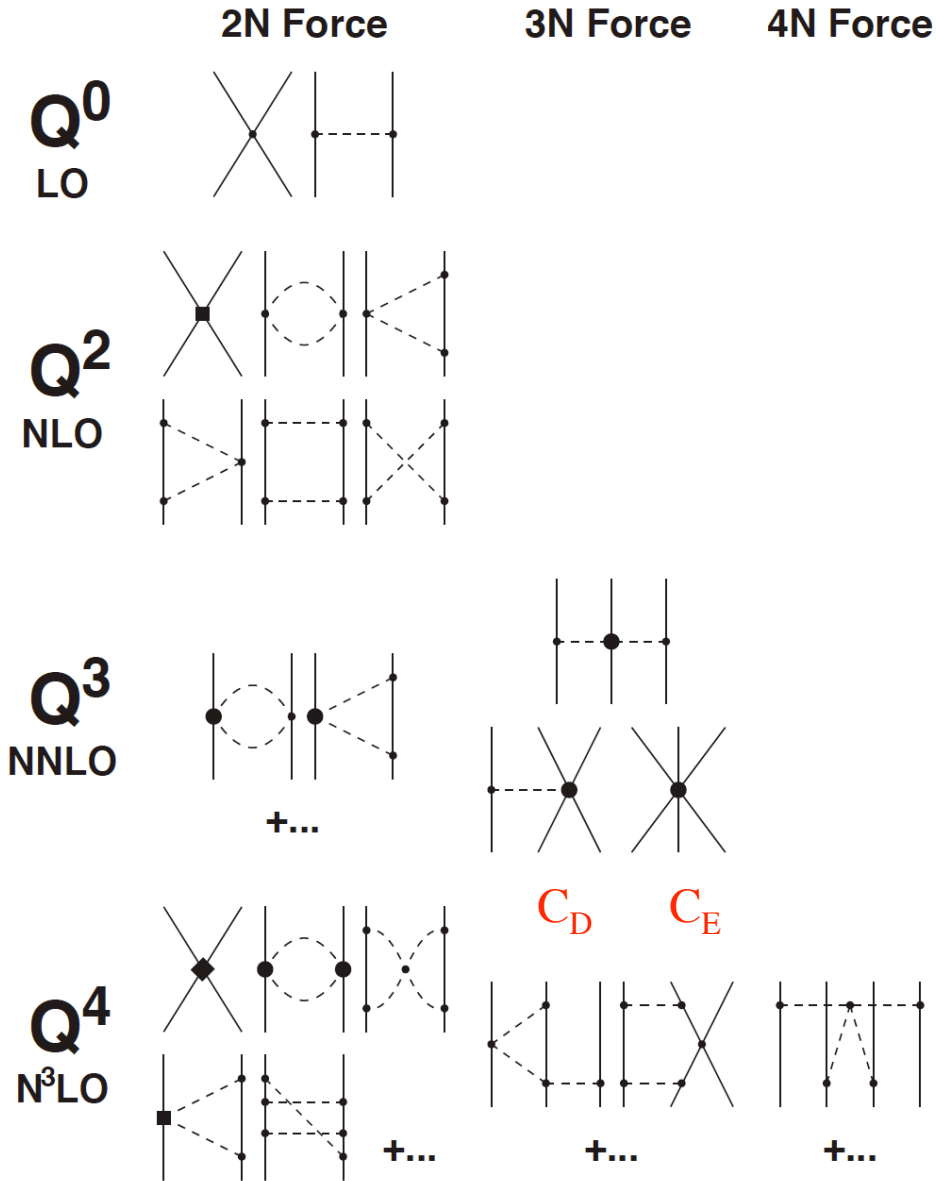
Main goal :

To arrive at a comprehensive description of all nuclei and low-energy reactions from the basic interactions between the constituent nucleons



Nuclear forces from chiral effective field theory

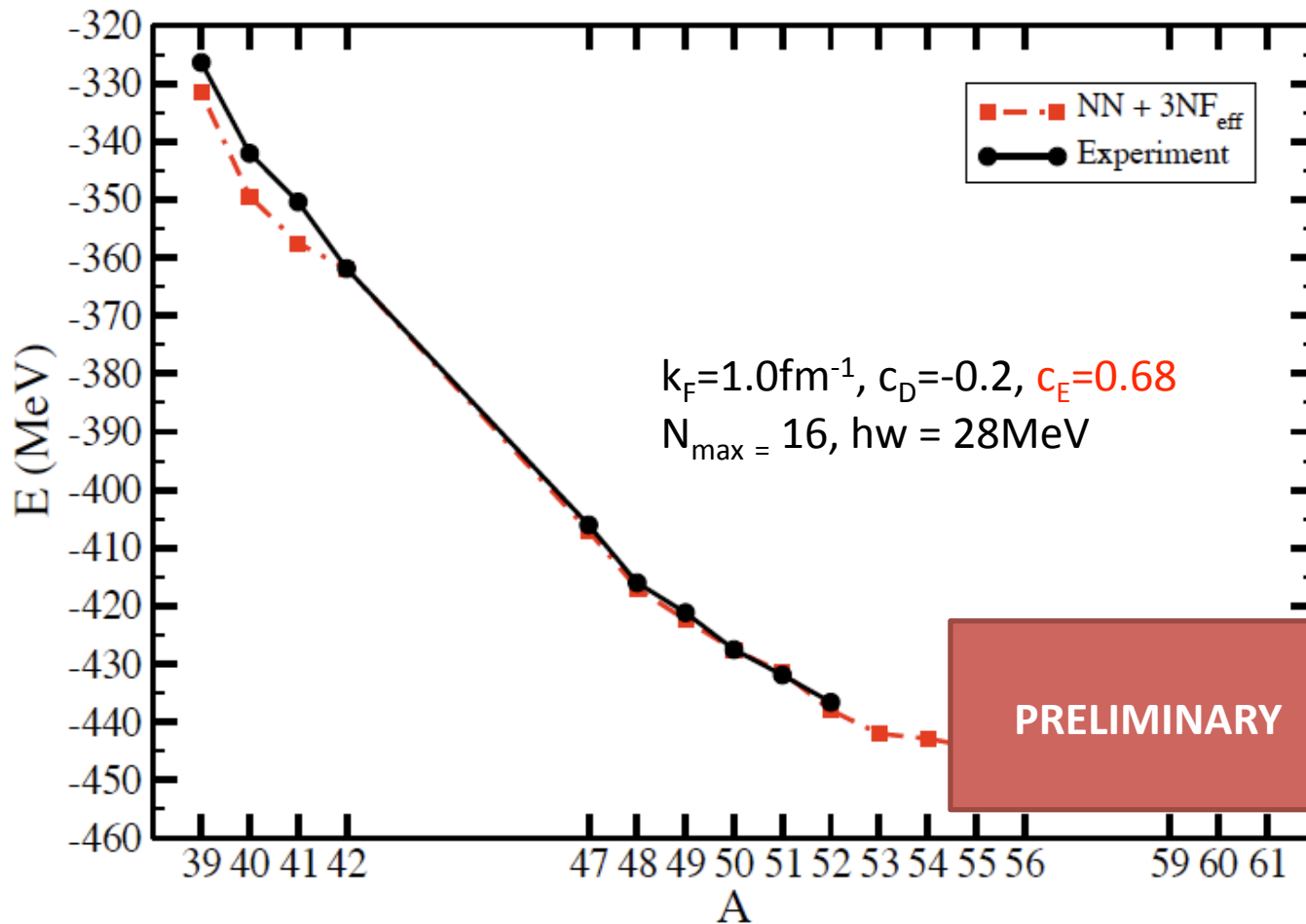
[Weinberg; van Kolck; Epelbaum *et al.*; Entem & Machleidt; ...]



[Epelbaum, Hammer, Meissner RMP 81, 1773 (2009)]

Low energy constants from fit of NN data, $A=3,4$ nuclei, or light nuclei.

Calcium isotopes from chiral interactions

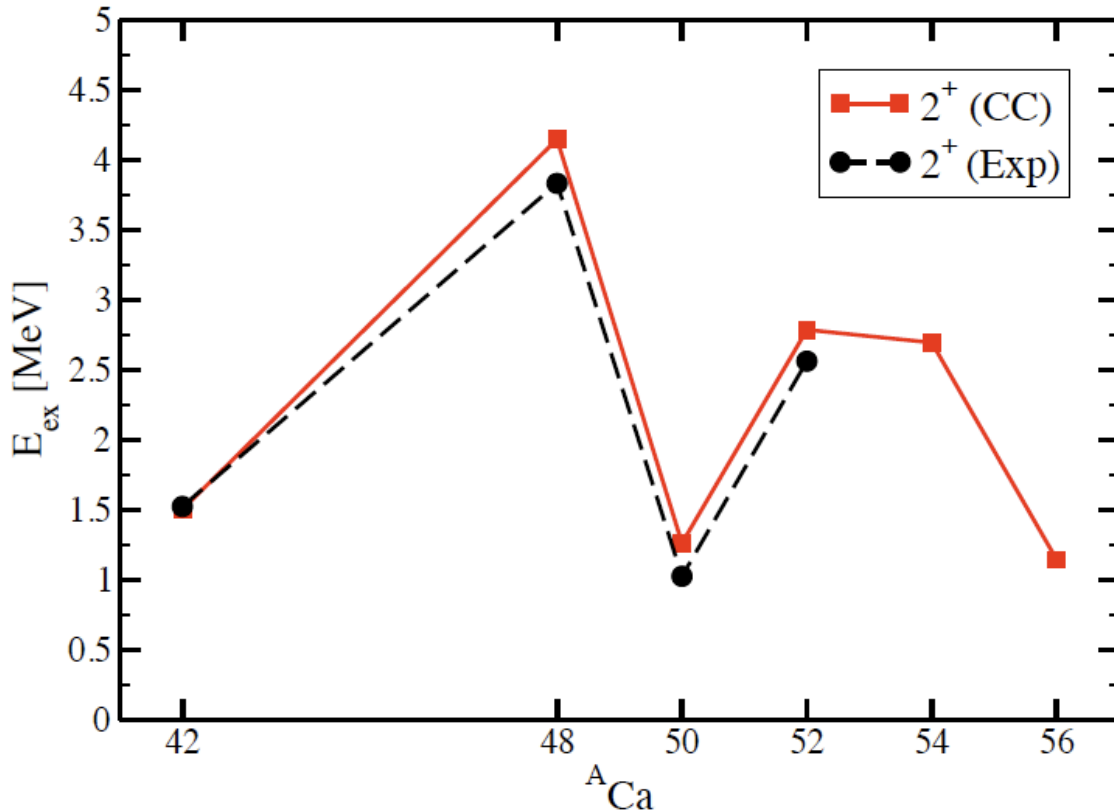


Main Features:

1. Total binding energies agree very well with experimental masses.
2. Masses for $^{40-52}\text{Ca}$ are converged in 17 major shells.
3. ^{60}Ca is not bound in 17 major shells.

[G. Hagen](#), [M. Hjorth-Jensen](#), [G. R. Jansen](#),
[R. Machleidt](#), [T. Papenbrock](#), in preparation (2012)

2⁺ systematics in Calcium isotopes from chiral interactions



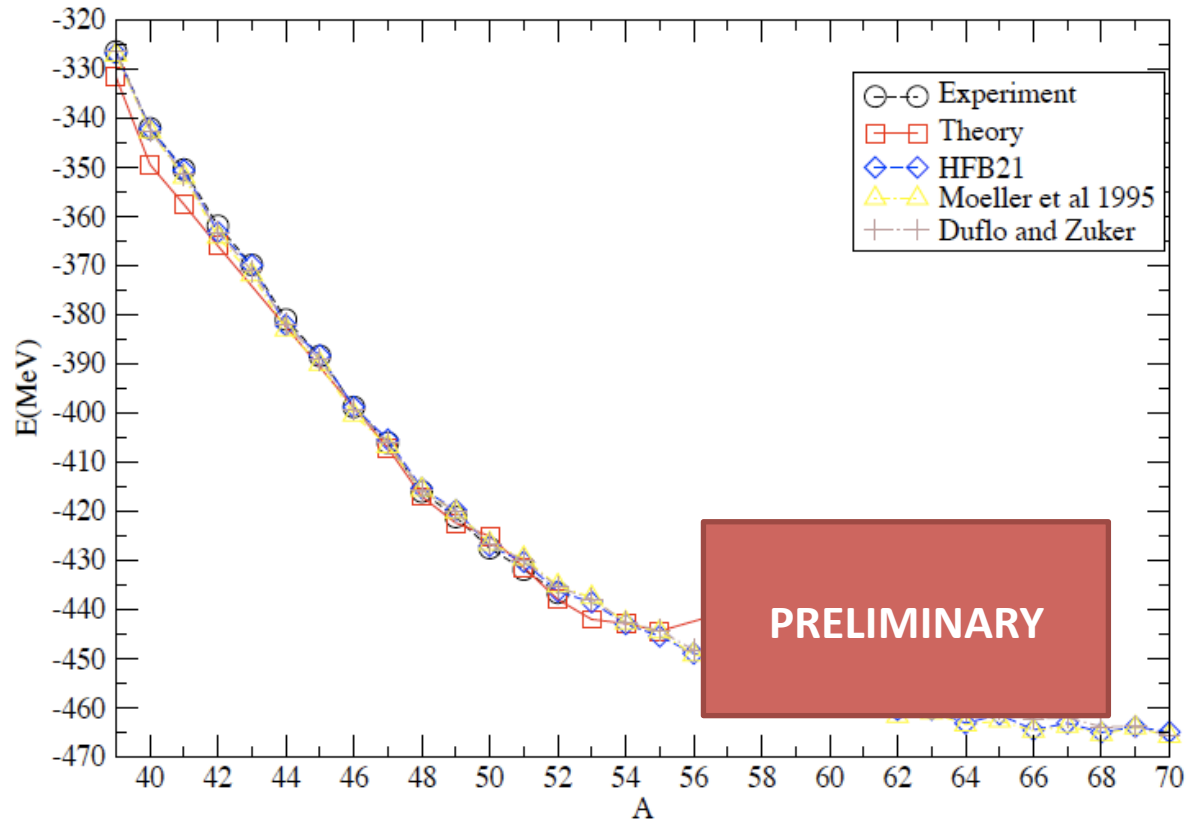
Main Features:

1. Very nice agreement between theory and experiment.
2. Our calculations for 2⁺ and 4⁺ in ⁵⁴Ca do not point to a new magic shell closure.

[G. Hagen](#), [M. Hjorth-Jensen](#), [G. R. Jansen](#), [R. Machleidt](#), [T. Papenbrock](#), in preparation (2012)

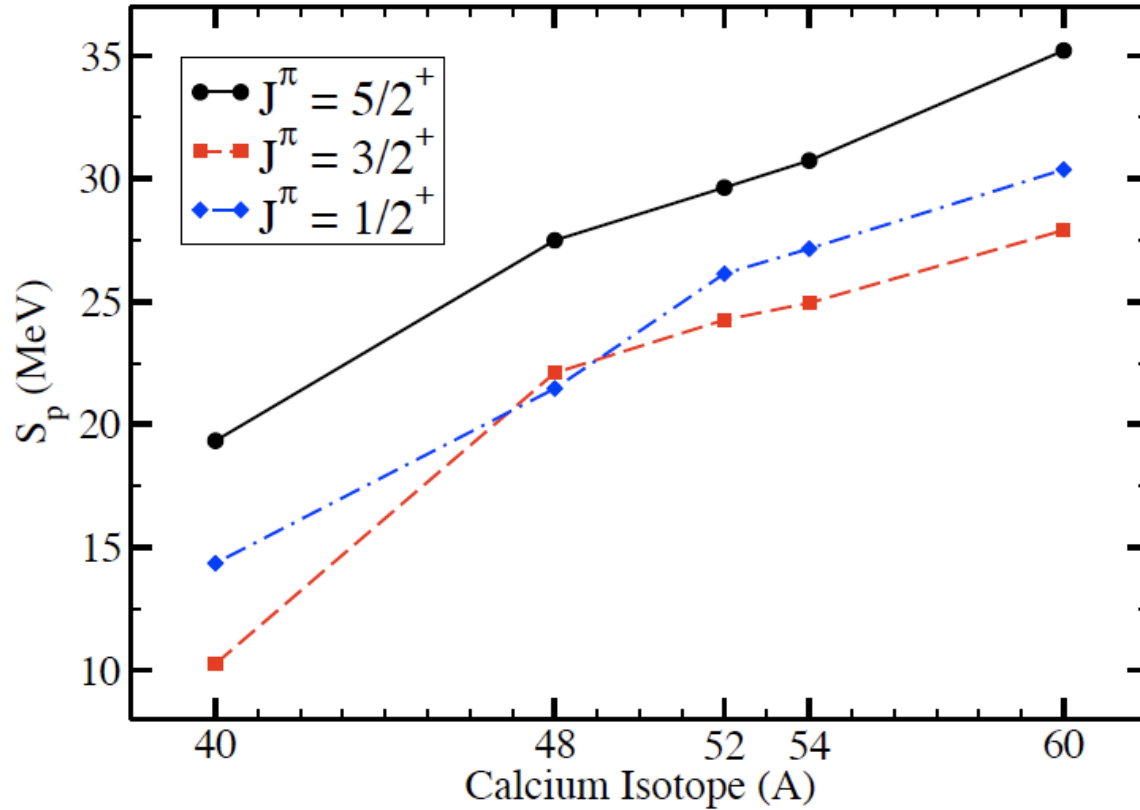
	⁴⁸ Ca			⁵² Ca			⁵⁴ Ca		
	2 ⁺	4 ⁺	4 ⁺ /2 ⁺	2 ⁺	4 ⁺	4 ⁺ /2 ⁺	2 ⁺	4 ⁺	4 ⁺ /2 ⁺
CC	4.148	4.675	1.13	2.787	5.349	1.92	2.696	5.827	2.16
Exp	3.833	4.503	1.17	2.563	?	?	?	?	?

Calcium isotopes from chiral interactions



1. Our calculations agree very well with available mass models for the the experimentally known Calcium isotopes.
2. Beyond ^{53}Ca masses are not known experimentally.
3. Can ab-initio structure calculations of masses put constraints on extrapolations?

Potassium isotopes from chiral interactions

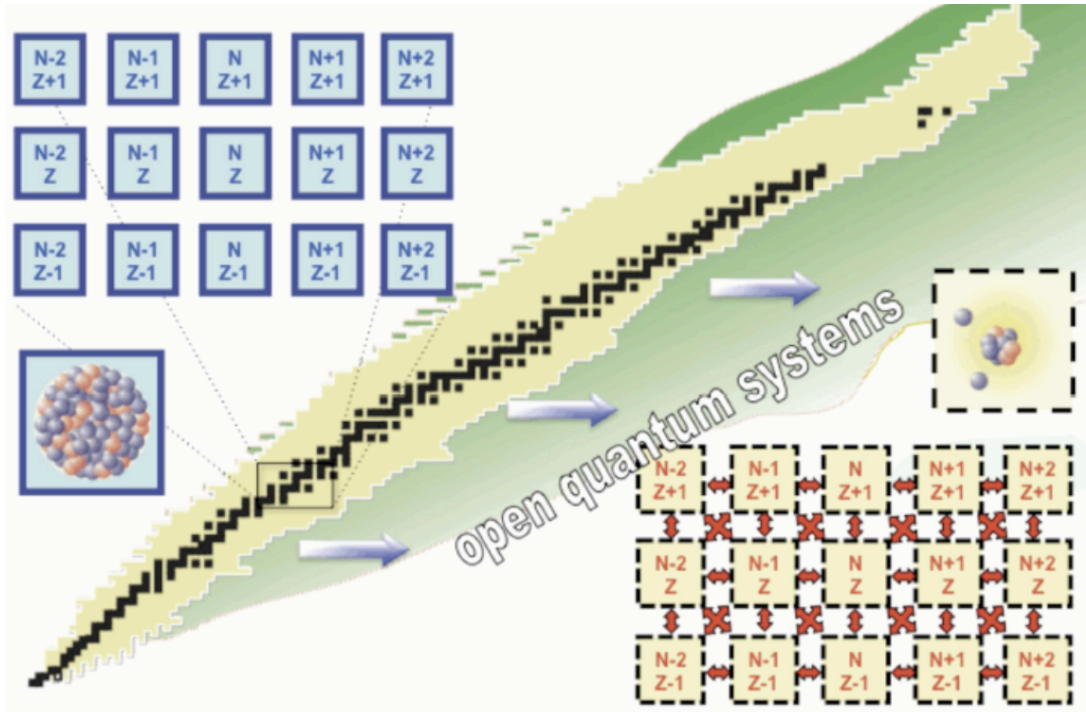


1. We reproduce level inversion in ^{47}K and get $1/2^+$ as the ground state.
2. We predict $3/2^+$ for the ground state in $^{51,53,59}\text{K}$.

$1/2^+$ state with respect to $3/2^+$ state in ^{39}K and ^{47}K .

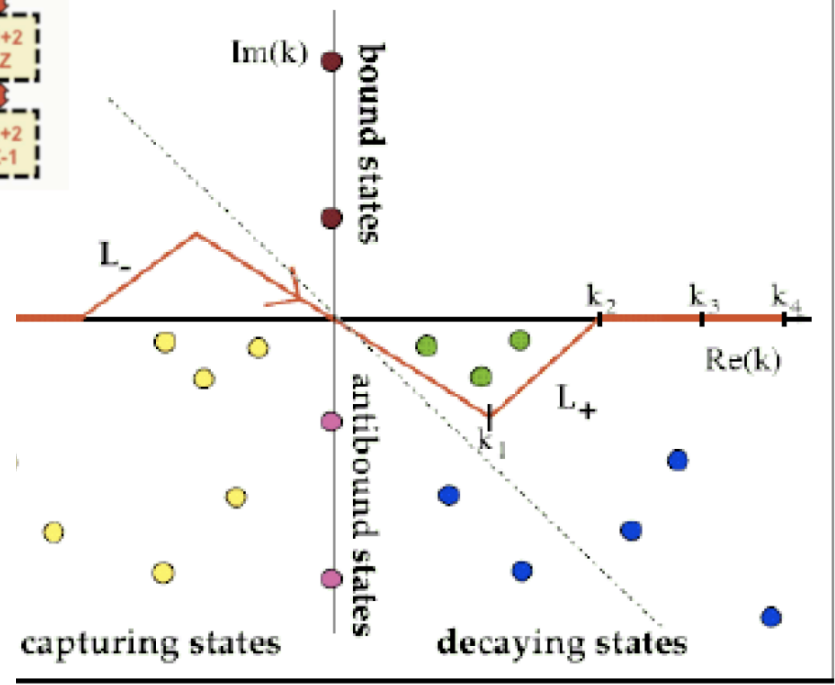
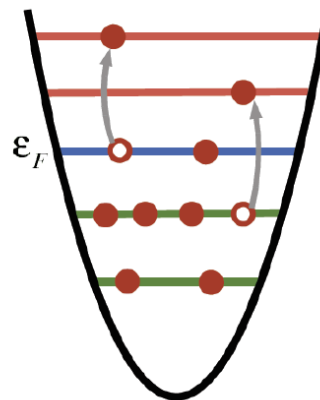
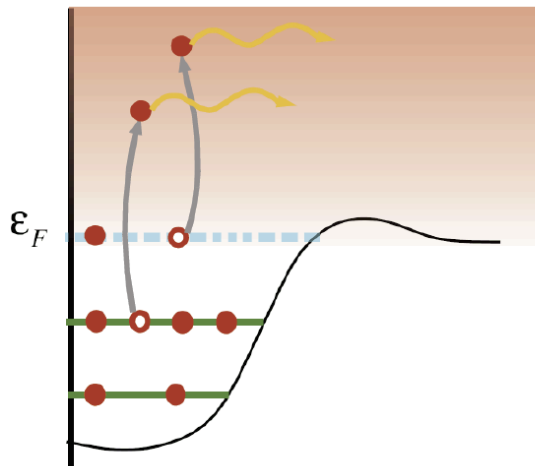
J^π	E(CC)	E(Exp)	E(CC)	E(Exp)
$3/2^+$	0.00	0.00	0.00	0.00
$1/2^+$	4.097	2.52	-0.636	-0.36

Open Quantum Systems



The Berggren completeness treats bound, resonant and scattering states on equal footing.

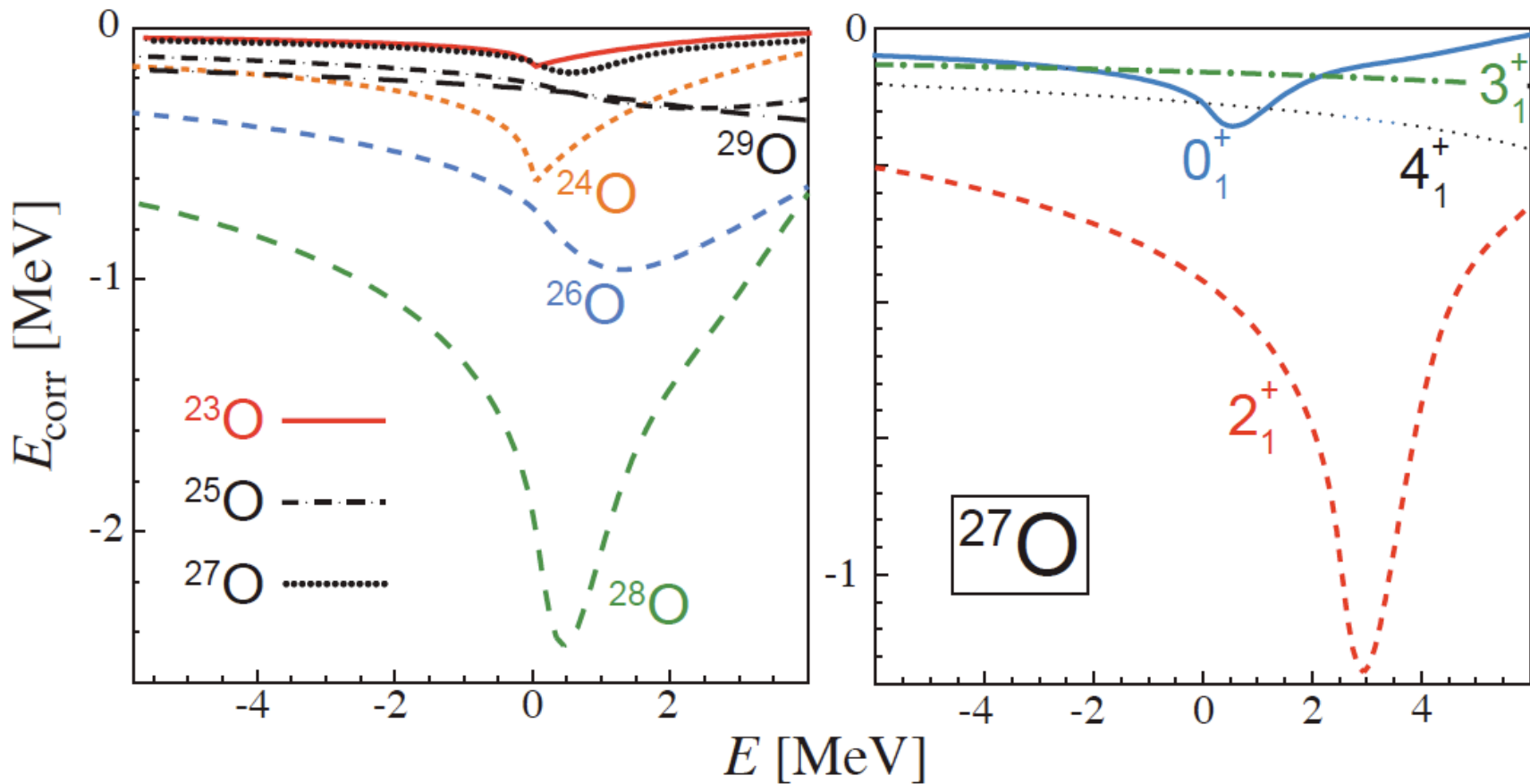
Has been successfully applied in the shell model in the complex energy plane to light nuclei. For a review see N. Michel et al J. Phys. G 36, 013101 (2009).



Continuum induced correlations

Continuum shell model calculations of oxygen isotopes. The effect of continuum correlations for nuclei with low neutron emission thresholds can be significant.

N. Michel et al, J. Phys. G **37** 064042 (2010).



Towards nuclear reactions with coupled-cluster theory

One-nucleon overlap functions

Elastic scattering, capture and transfer reactions of a nucleon on/to a target nucleus with mass A is determined by the one-nucleon overlap function

$$O_A^{A+1}(lj; r) = \langle A \parallel \tilde{a}_{lj}(r) \parallel A + 1 \rangle = \sum_n \langle A \parallel \tilde{a}_{nlj} \parallel A + 1 \rangle \phi_{nlj}(r)$$

Microscopic definition of Spectroscopic Factors

SF is the norm of the overlap function and quantifies the degree of correlations
SFs are not observables and depend on the resolution scale

$$SF = \int_0^\infty dr r^2 |O_A^{A+1}(lj; r)|^2$$

Asymptotic properties of the one-nucleon overlap functions

The overlap functions satisfy a one-body Schrodinger like equation, and outside the range of the interaction the overlap function is proportional to a single-particle wave function

$$O_A^{A+1}(lj; r) = C \frac{e^{-\kappa r}}{\kappa r}$$

Bound states

$$O_A^{A+1}(lj; r) = A(j_l(kr) - \tan \delta_l n_l(kr))$$

Scattering states

Asymmetry dependence and spectroscopic factors

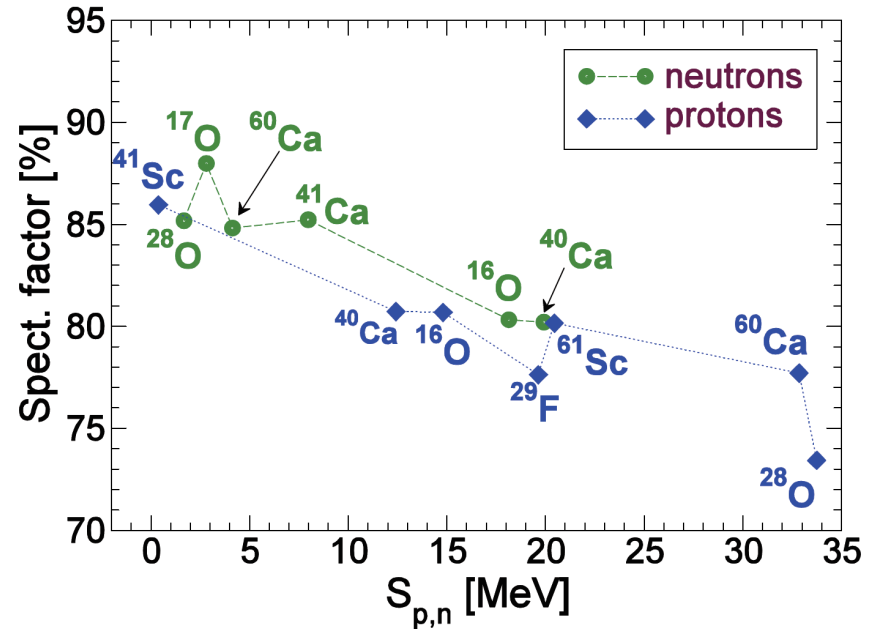
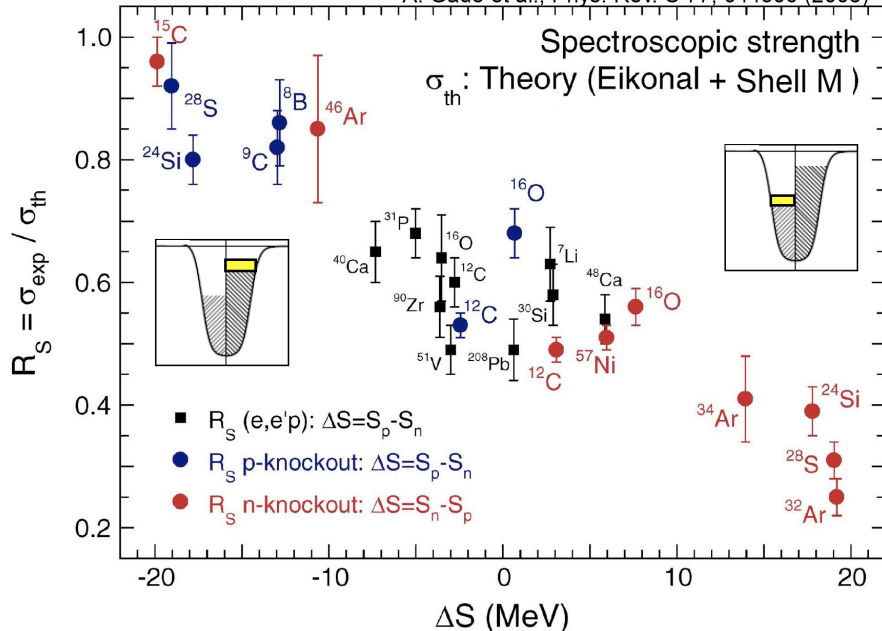
- Spectroscopic factors are not observables
- They are extracted from a cross section based on a specific structure and reaction model
- Structure and reaction models need to be consistent!

Theoretical cross section:

$$\sigma(j^\pi) = \left(\frac{A}{A-1}\right)^N C^2 S(j^\pi) \sigma_{sp}(j, S_N + E_x[j^\pi])$$

Reaction theory
Structure theory

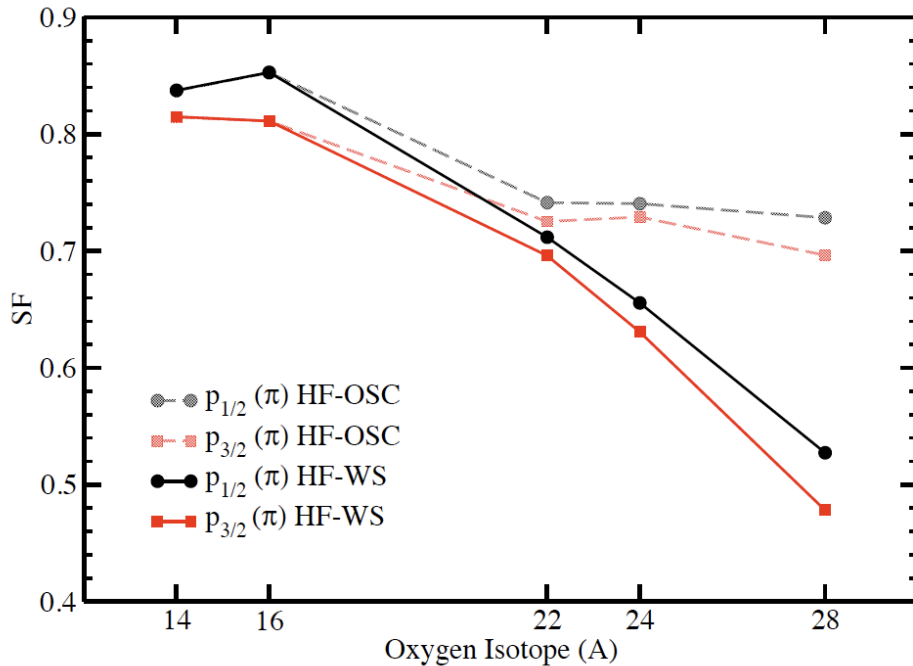
A. Gade et al., Phys. Rev. C 77, 044306 (2008)



C. Barbieri, W.H. Dickhoff, Int. Jour. Mod. Phys. A24, 2060 (2009).

Self-consistent green's function method show rather weak asymmetry dependence for the spectroscopic factor.

Quenching of spectroscopic factors for proton removal in neutron rich oxygen isotopes



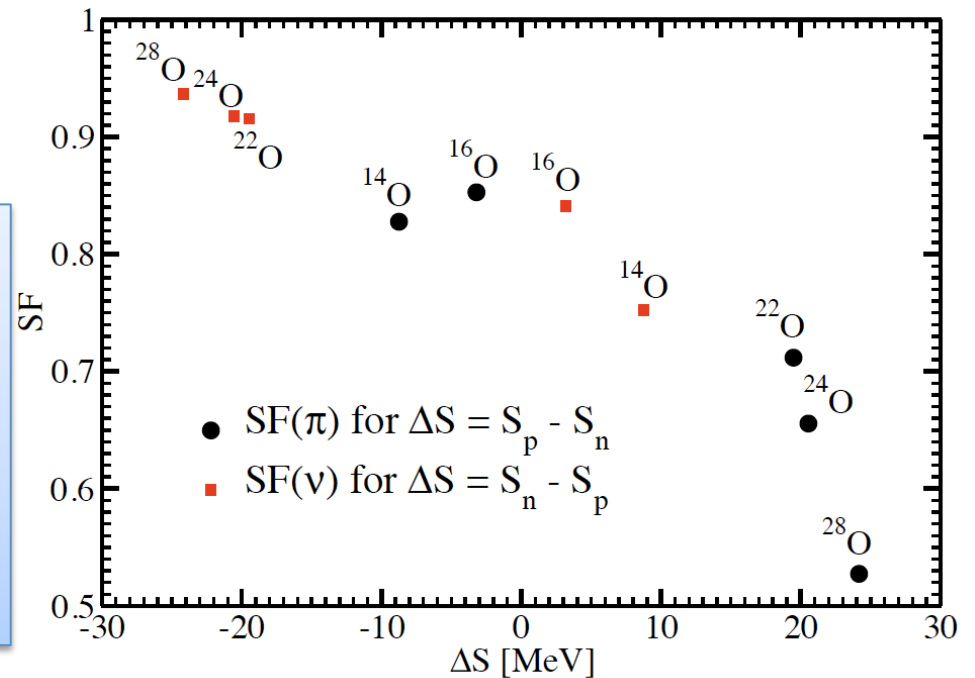
Spectroscopic factor is a useful tool to study correlations towards the dripline.

SF for proton removal in neutron rich ^{24}O show strong “quenching” pointing to large deviations from a mean-field like picture.

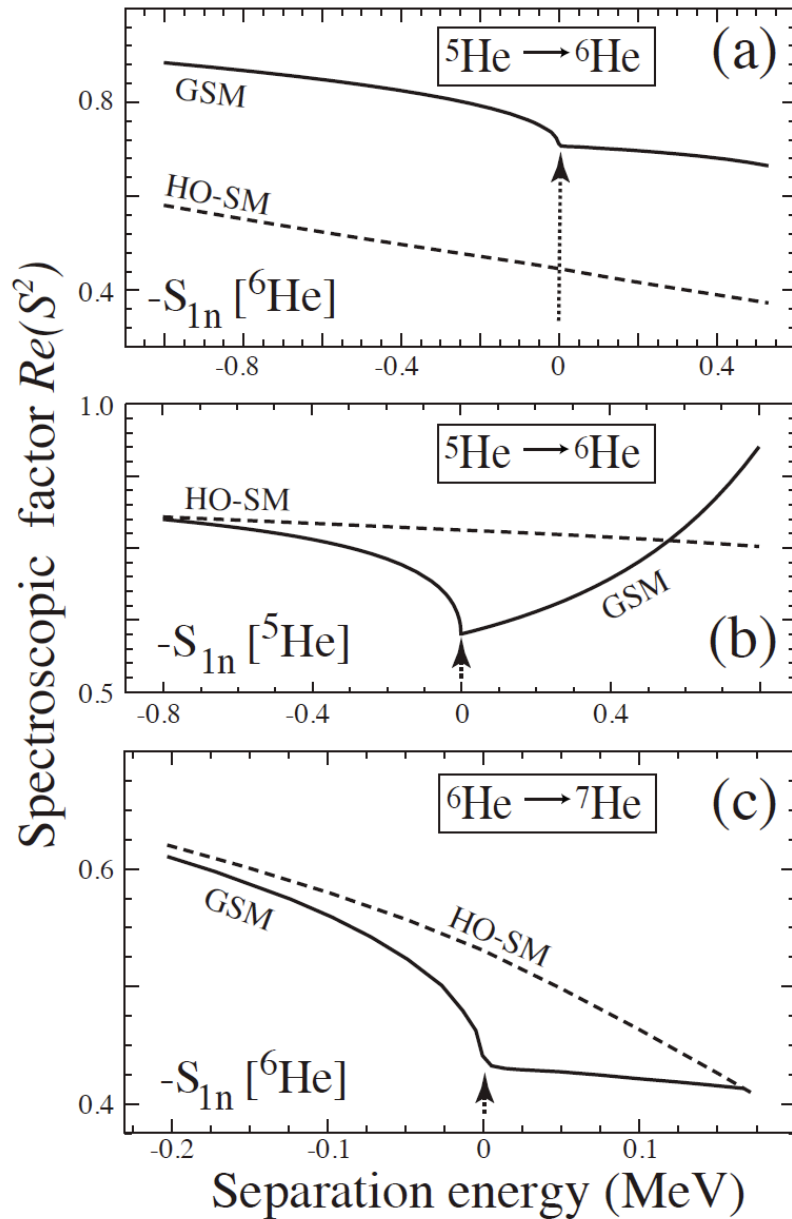
G. Hagen et al Phys. Rev. Lett. 107, 032501 (2011).

Strong asymmetry dependence on the SF for proton and neutron removal in neutron rich oxygen isotopes.

SF~1 for neutron removal while protons are strongly correlated SF ~0.6-0.7 in $^{22,24,28}\text{O}$



Threshold effects and spectroscopic factors



Near the scattering threshold for one-neutron decay the spectroscopic factors are significantly influenced by the presence of the continuum. The standard shell model

$$\langle \Psi_A^{J_A} || a_{nlj}^+ || \Psi_{A-1}^{J_{A-1}} \rangle^2$$

approximation to spectroscopic factors completely fails in this region.

N. Michel et al Phys. Rev. C **75**, 031301 (2007)

N. Michel et al Nucl. Phys. A **794**, 29 (2007)

Top and middle:

$$\langle {}^6\text{He}(\text{g.s.}) | [{}^5\text{He}(\text{g.s.}) \otimes p_{3/2}]^{0^+} \rangle$$

Bottom :

$$\langle {}^7\text{He}(\text{g.s.}) | [{}^6\text{He}(\text{g.s.}) \otimes p_{3/2}]^{0^+} \rangle$$

Treatment of long-range Coulomb effects

We diagonalize the one-body Schrödinger equation in momentum space using the off-diagonal method described in

N. Michel Phys. Rev. C 83, 034325 (2011)

$$h = \frac{\hat{p}^2}{2m} - V_o \left[1 + \exp\left(\frac{r - R_0}{d}\right) \right]^{-1} + U_{Coul}(r)$$

N_{GL}	E cut (MeV)	Γ cut (keV)	E sub (MeV)	Γ sub (keV)	E off-diag (MeV)	Γ off-diag (keV)
15	0.461875	-11.6596	0.464574	9.19011	0.46396	10.2211
30	0.465707	13.4833	0.463777	8.26812	0.463343	8.97219
45	0.463476	8.71097	0.463709	8.33267	0.463334	8.96171
60	0.463307	8.68396	0.463681	8.36454	0.463329	8.96458
75	0.463227	8.70558	0.463667	8.38006	0.463328	8.96595
90	0.46284	8.88896	0.463659	8.3888	0.463327	8.96669
105	0.462952	8.69106	0.463654	8.39421	0.463326	8.96712
120	0.462949	8.62468	0.46365	8.3978	0.463326	8.9674
exact	0.463324	8.96828	0.463324	8.96828	0.463324	8.96828

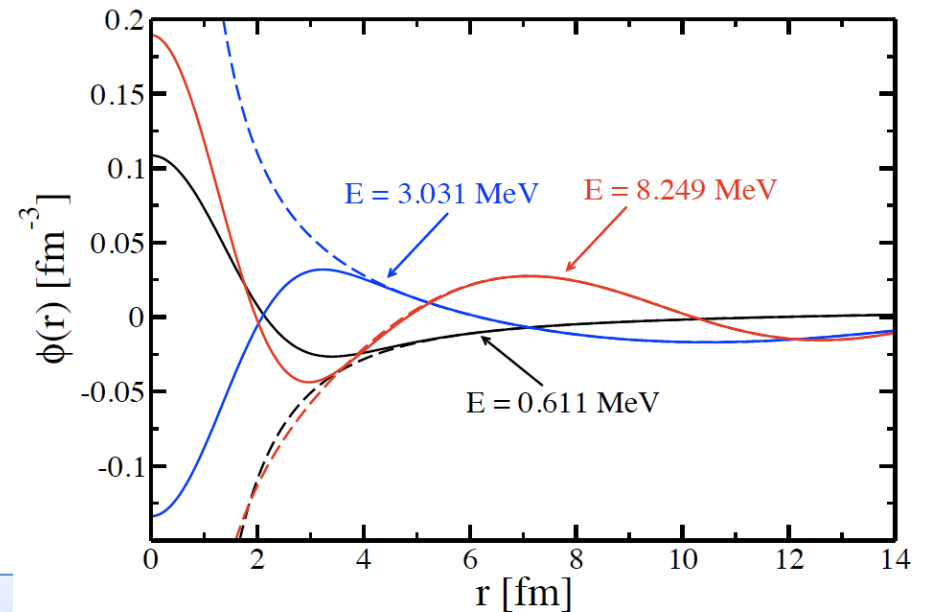
The many-nucleon Hamiltonian is

$$H = \hat{T} - \hat{T}_{cm} + \hat{V}_{NN} + V_{Coul}$$

We write the Coulomb interaction as a sum of two terms:

$$V_{Coul} = U_{Coul}(r) + [V_{Coul} - U_{Coul}(r)].$$

The second term is short range and can be expanded in Harmonic Oscillator basis. The first term contains the long range Coulomb part.



Elastic proton/neutron scattering on ^{40}Ca

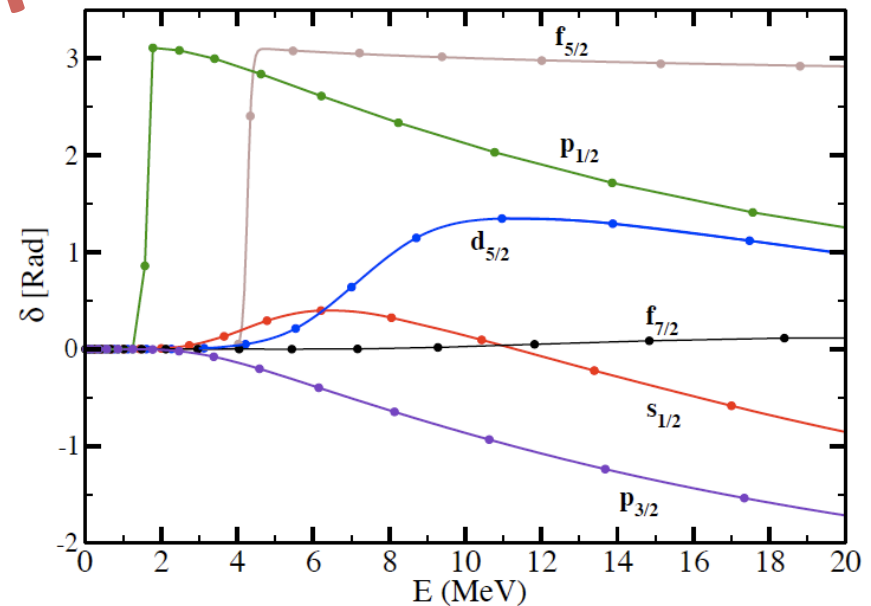
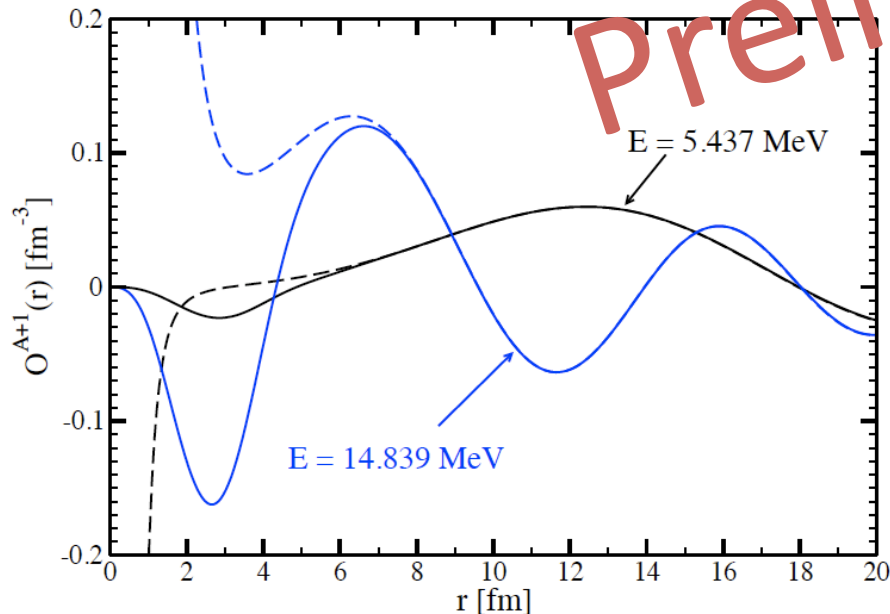
The one-nucleon overlap function: $O_A^{A+1}(lj; kr) = \int_n \langle A+1 \parallel \tilde{a}_{nlj}^\dagger \parallel A \rangle \phi_{nlj}(r)$.

Beyond the range of the nuclear interaction the overlap functions take the form:

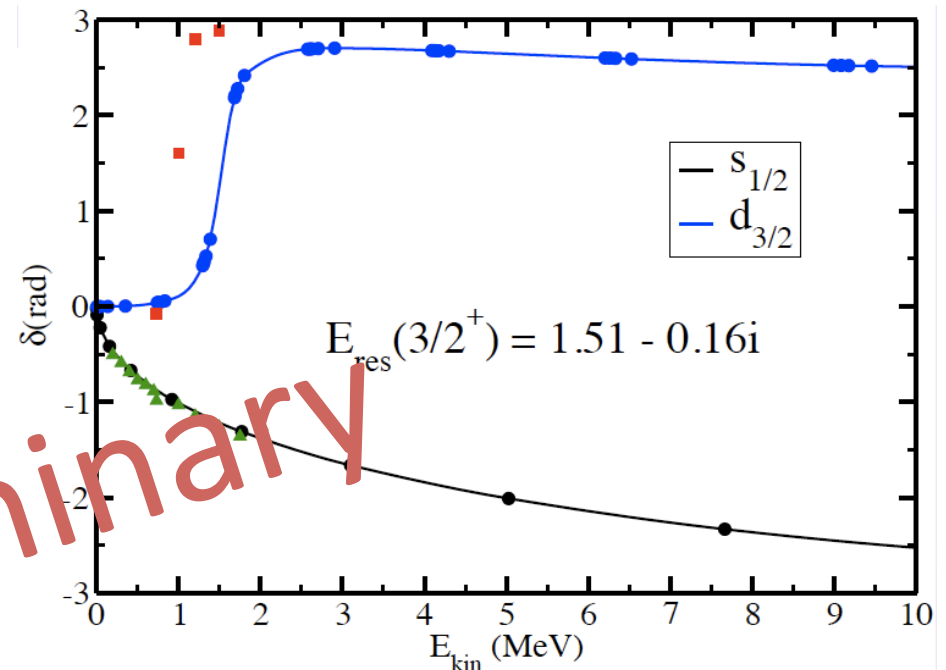
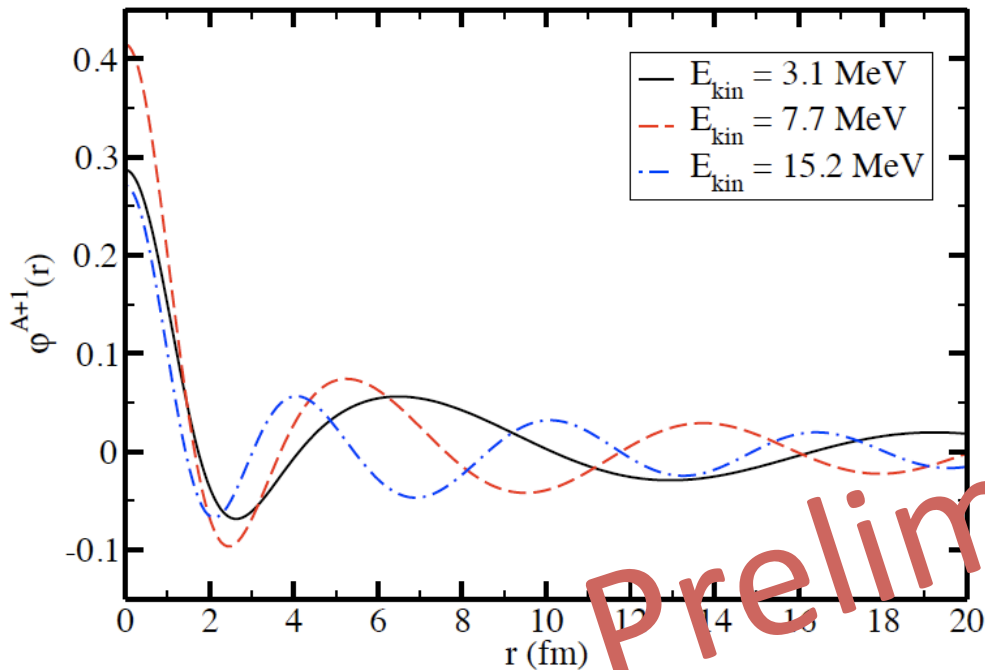
$$O_A^{A+1}(lj; kr) = C_{lj} \frac{W_{-\eta, l+1/2}(kr)}{r}, \quad k = i\kappa$$

$$O_A^{A+1}(lj; kr) = C_{lj} [F_{l,\eta}(kr) - \tan \delta_l(k) G_{l,\eta}(kr)]$$

G. Hagen and N. Michel,
in preparation (2012).



Elastic scattering phase shifts for neutrons on ^{16}O with coupled-cluster theory



Overlap functions provides a simple and intuitive picture of reactions

Left figure: One neutron overlap functions for various $J = 1/2^+$ scattering states in ^{17}O using SRG evolved interaction with cutoff $\lambda = 2.66 \text{ fm}^{-1}$

Right figure: By matching the known asymptotic form of the overlap functions to scattering solutions we can extract low-energy elastic scattering phase shifts.

Densities and radii from coupled-cluster theory

We solve for the right and left ground state of the similarity transformed Hamiltonian

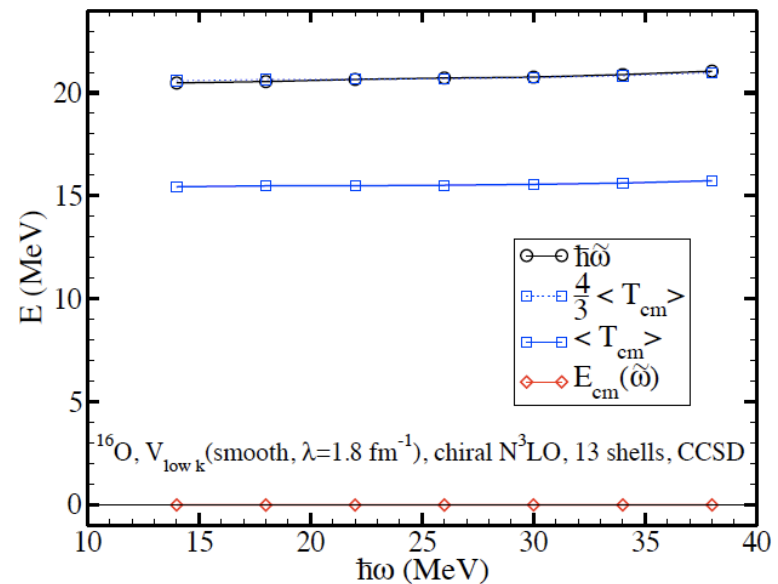
$$e^{-T} H_N e^T |\phi_0\rangle = \overline{H}_N |\phi_0\rangle = E_{CC} |\phi_0\rangle \quad \langle \phi_0 | L_0 \overline{H}_N = E_{CC} \langle \phi_0 | L_0$$

The density matrix is computed within coupled-cluster method as:

$$\rho_{pq} = \langle \Psi_0 | a_p^\dagger a_q | \Psi_0 \rangle = \langle \phi_0 | L e^{-T} a_p^\dagger a_q e^T | \phi_0 \rangle = \langle \phi_0 | L a_p^\dagger a_q | \phi_0 \rangle$$

The coupled-cluster wave function factorizes to a good approximation into an intrinsic and center of mass part, $\Psi = \psi_{in} \Gamma$ where the center of mass part is a Gaussian with a fixed oscillator frequency independent of single-particle basis

GH, T. Papenbrock and D. Dean et al, Phys. Rev. Lett. **103**, 062503 (2009)



We can obtain the intrinsic density by a deconvolution of the laboratory density

B. G. Giraud, Phys. Rev. C **77**, 014311 (2008)

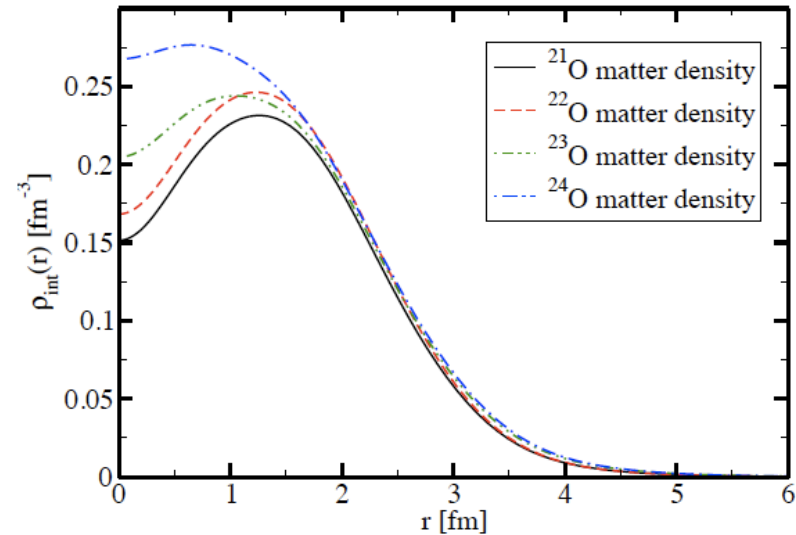
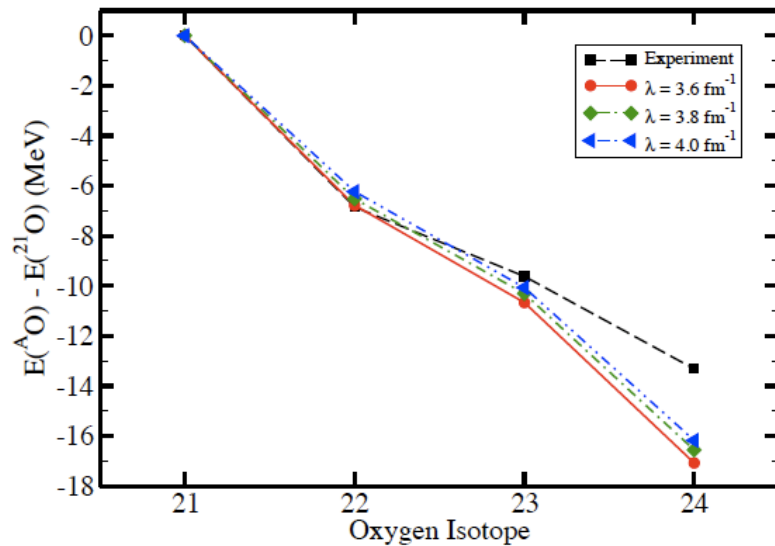
$$A^{-1} \rho(r) = A^{-1} \int dR [\Gamma(R)]^2 \sigma \left[\frac{A}{A-1} (r-R) \right]$$

Lab. density

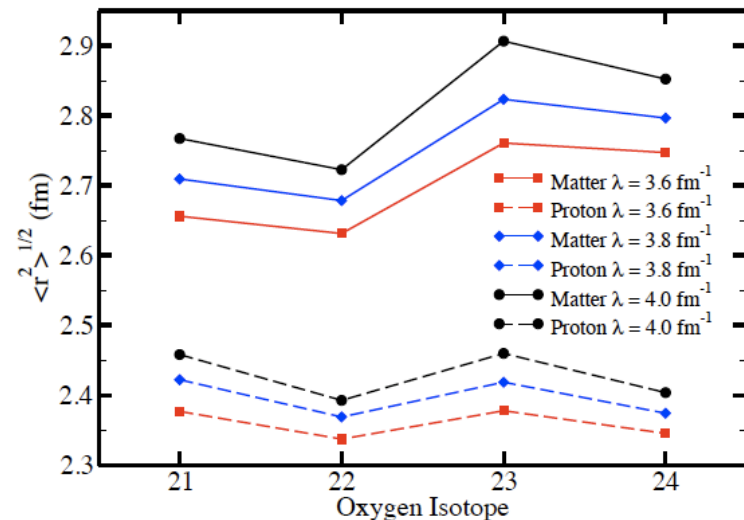
Center of mass part

Intrinsic density

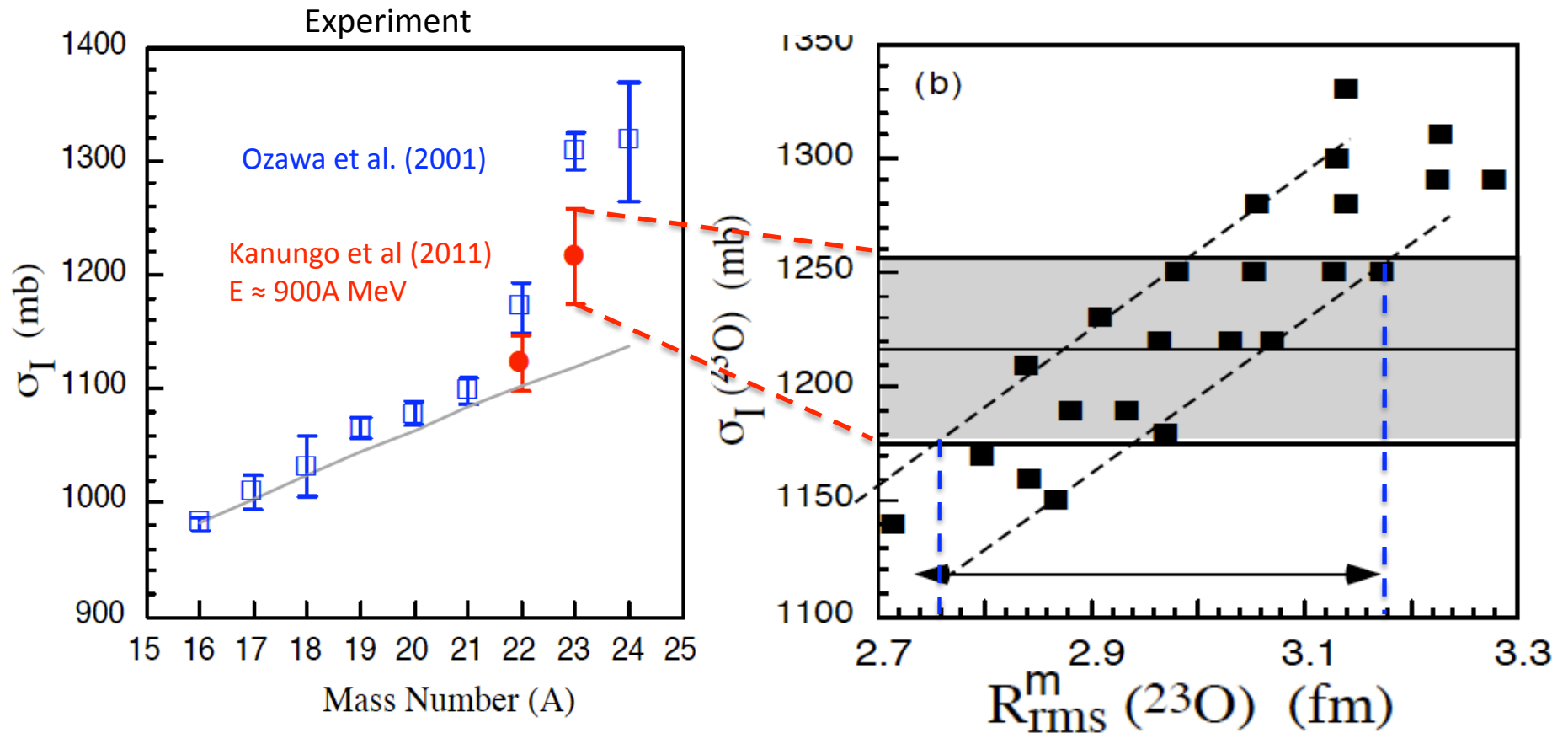
Densities and radii from coupled-cluster theory



1. Relative energies in $^{21-24}\text{O}$ depend weakly on the resolution scale
2. We clearly see shell structure appearing in the matter densities for $^{21-24}\text{O}$
3. Matter and charge radii depend on the resolution scale, however relative difference which is relevant for isotope shift measurements does not



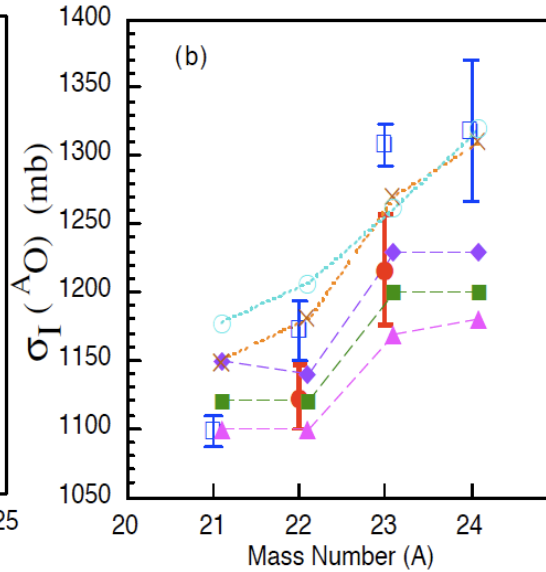
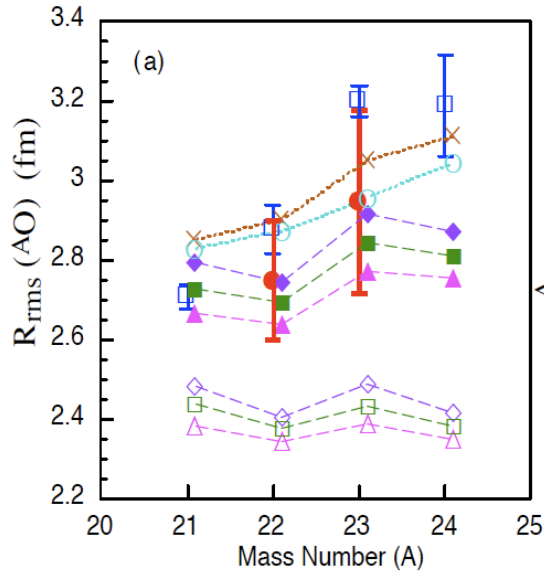
^{23}O interaction cross section (scattering off ^{12}C target @ GSI)



Experimental radii extracted from matter distribution within Glauber model.
Main result of new measurement: ^{23}O follows systematics; interaction cross section consistent with separation energies.

R. Kanungo *et al* Phys. Rev. C **84**, 061304 (2011)

Resolving the anomaly in the cross section of ^{23}O



The anomaly of ^{23}O

New measurements (R. Kanungo) of the ^{23}O cross section and coupled cluster calculations show that ^{23}O is not consistent with a one-neutron halo picture

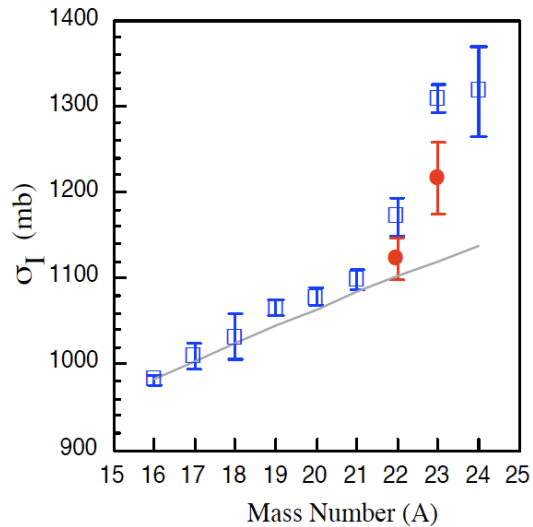


TABLE I: Measured interaction cross sections and the root mean square point matter radii (R_{rms}^m (ex.)) for $^{22-23}\text{O}$.

Isotope	$\sigma_I(\Delta\sigma)$ (mb)	$\Delta\sigma(\text{Stat.})$ (mb)	$\Delta\sigma(\text{Syst.})$ (mb)	R_{rms}^m (ex.) (fm)
^{22}O	1123(24)	18.5	15.3	2.75 ± 0.15
^{23}O	1216(41)	33.1	24.7	2.95 ± 0.23

Summary and outlook

1. CC calculations for oxygen and calciums with effects of 3NF and continuum are promising. Significant improvement in binding energy and spectra.
2. Quenching of spectroscopic factors near neutron dripline show role of continuum induced correlations for protons
3. Promising results for elastic nucleon-nucleus scattering on ^{40}Ca and ^{16}O
4. Densities and cross sections from coupled-cluster theory help resolve long-standing anomaly of ^{23}O
5. Isotopic shift in radii of oxygen isotopes well reproduced with chiral NN interactions